From collectivity to the single-particle picture in the photoionization of clusters

Olaf Frank and Jan M. Rost
Fakultät für Physik, Universität Freiburg, Hermann-Herder-Strasse 3, D-79104 Freiburg, Germany and Institue for Nuclear Theory, University of Washington, Box 351550, Seattle, Washington 98195
(Received 25 August 1998)

Photoionization of alkali-metal clusters is investigated theoretically for different photon energy regimes. At low energies the photo cross section is characterized by the well-known plasmon peak resulting from collective electron dynamics. For high energies the ionization cross section exhibits an oscillatory behavior, which can be explained by single-particle effects. In this paper we use the random phase approximation (RPA) to calculate the photo cross section on an equal footing for both, the low- and the high-energy regime. Thereby, we can show that the cross sections for photoionization calculated in the collective RPA and in the single-particle picture indeed merge for high photon energies. Moreover, we demonstrate that the oscillatory behavior can already be identified at low photon energies where the cross section is not yet exponentially small. Hence, it should be possible to identify the oscillations experimentally. [S1050-2947(99)07706-9]

PACS number(s): 36.40.Gk, 33.80.−b, 21.60.Jz

I. INTRODUCTION

Since the beginning of cluster physics in the late 1970s the irradiation with laser light has revealed fundamental cluster properties [1,2]. One of the important characteristics is the collective response of the valence electron cloud to laser radiation. The most prominent consequence of this collective behavior in the absorption spectrum is the occurrence of the giant dipole resonance that accounts for almost the entire oscillator strength. This resonance, which can be excited in most cases with visible laser light corresponding to an energy of a few electron volts, was investigated thoroughly in experimental regard [2,3]. Theoretically, it can be described quite well within the random-phase approximation (RPA) or the time-dependent local-density approximation (TDLDA), see, for example, [1,4,5]. From this work one can conclude that the observed behavior of the clusters is mostly due to the dynamics of the valence electrons with the collective nature of the response to linear perturbations of the ground state playing a key role.

While the vast majority of publications deals with the energy regime close to the giant dipole resonance, little attention has been devoted to higher photon energies, e.g., to the photoionization well beyond the ionization potential [6,7]. Our analysis of this regime under the assumption of the validity of the effective single-particle picture has revealed an expected exponential decrease of the cross section as a function of photon energy superimposed with an unexpected oscillatory structure [6]. We argued that at very high-photon energies the single-particle picture should give reasonable results since the valence electron cloud is too inert to follow the rapid oscillations of the electromagnetic field. Therefore, the electron density within the cluster would not be altered significantly and the effective perturbing potential should equal the external potential represented by the laser field.

While this argument certainly applies to the limit of high-photon energies one cannot say *a priori* for which finite energies it is already valid. However, for the oscillations to be an effect observable in the experiment, it is crucial that they can be identified already at photon energies that are lower than those for which the first innershell ionization processes occur since the latter dominate the ionization cross section.

To our knowledge, no measurements of the photoionization cross section of alkali-metal clusters for an energy interval large enough to reveal one cycle of the oscillatory structure have been performed. For alkali-metal clusters with up to 100 constituents such a measurement requires covering an interval of approximately 5 eV in the regime of synchrotron radiation [6].

However, analogous experiments have been performed for the photoionization cross sections of C_{60} [8] and C_{70} [9]. There, an oscillatory structure has been found, which is consistent with our calculation in the single-particle picture [7], see also [10]. Hence, in this case the single-particle approach seems to be reasonable at photon energies of the order of 10^2 eV, which is approximately twice the energy of the plasmon resonance in C_{60}.

Another possibility to observe the oscillations, although very difficult to realize experimentally, is the measurement of the differential electron-impact ionization of clusters as shown by Keller *et al.* [11].

The goal of this paper, calculating the photo cross section within an RPA approach, is twofold: First, to confirm the oscillatory behavior of the cross section which was discovered using an effective single-particle approach only. Second, to investigate, how the low-energy (collective) signature of the cross section merges into the single-particle dominated high-energy behavior. As a result, we will demonstrate that it should be possible to identify the oscillations in the experiment.

The paper is organized as follows. The first part of Sec. II contains a short summary of the results of the semiclassical analysis of the cross section for photoionization in the single-particle picture from [6]. In the second part of Sec. II the methods, which account for the influence of collective effects (RPA, TDLDA), are briefly reviewed and the approach used in this paper is explained. In Sec. III the results of the single-particle calculation are compared to the results of

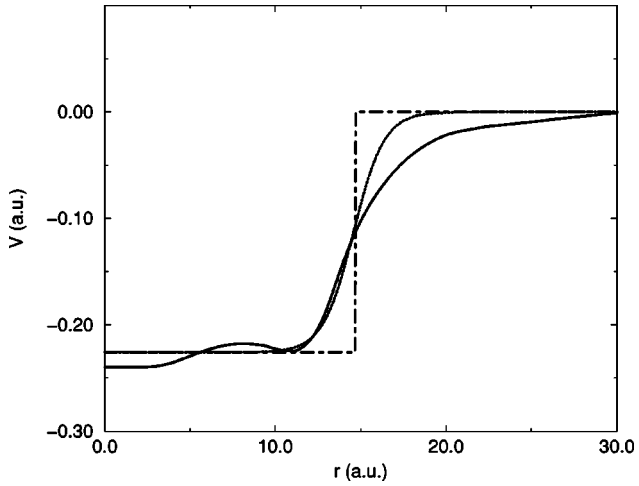

FIG. 1. Effective cluster potentials for Na_{34} from a DFT calculation by Ekardt [13] (solid line) and from Eq. (1) with parameters $V_0=0.226$, $L=14.478$, and $a=0.9$ (dash-dotted line). In addition, a box potential with equivalent range L and depth V_0 is shown.

RPA calculations for the same test system, Na_{34}. The paper ends with a conclusion in Sec. IV.

II. THEORY

The description of physical properties of clusters is due to the high number of degrees of freedom, a major problem. A drastic approximation is to neglect the ionic structure of the cluster and to assume that the valence electrons of the atoms move freely in the homogeneously distributed background charge density of the ionic cores. This approximation, known as jellium model, has proven to work well in the case of alkali-metal clusters [1,2]. The ionic charge density is distributed over the volume of the cluster and its integral gives the total charge of the ions. For the ground state of the cluster the valence electron density can be calculated using density-functional theory (DFT) [12]. A set of trial wave functions is obtained, which are the solutions of a single-particle Schrödinger equation with an effective single-particle potential that contains the interaction among the valence electrons. This approach was introduced successfully to alkali-metal clusters by Ekardt [13]. To some approximation the trial wave functions may be interpreted as the single-particle wave functions [19].

The effective potential of Na_{34} from a calculation by Ekardt [13] is shown in Fig. 1 along with the Woods-Saxon potential,

$$V_{WS}=\frac{-V_0}{1+\exp[a(r-L)]}, \tag{1}$$

which will be used for the semiclassical analysis of the single-particle cross section. The depth of the Woods-Saxon potential is given by V_0 and a determines the steepness of the cluster edge, which defines the cluster radius L. V_0, L, and a are chosen in such a way that they approximate the effective single-particle potential from the DFT calculation.

The essential features of the potential, i.e., a flat interior and a pronounced rise at the cluster edge, are similar in both potentials and they are found to mainly influence the overall behavior of the cross section for photoionization as a function of photon energy. From these potentials the cross section for photoionization can be calculated, either in the single-particle picture, or including the collective behavior of the valence electrons. For both cases we can use the same initial- and final-state wave functions since within an RPA approach the collective response of the electron cloud to the laser field can be described with an effective dipole operator V_{eff} whose form we will derive below.

For a spherical potential as in Eq. (1) the total photoionization cross section is the sum of the partial ionization cross section for transitions $l'\rightarrow l$ between eigenstates ψ of the single-particle Hamiltonian with angular momentum l,l'. Assuming unpolarized light, including summation over all final magnetic states m_f and averaging over the initial magnetic states m_i [14], such a partial cross section reads (atomic units are used throughout the paper)

$$\sigma_{El\leftarrow n'l'}(\omega)=\omega(2\pi)^2\alpha_F\frac{l_>}{2l'+1}|\langle\psi_{El}(r)|D|\psi_{n'l'}(r)\rangle_r|^2, \tag{2}$$

where $D=D(r)$ is the radial dipole operator, $l_>$ is $\max(l',l)$, n' is the principal quantum number of the initial state, and E is the energy of the final state in the continuum.

A. Independent particle approach and semiclassical results

For the independent particle picture the dipole operator represents the usual perturbation $V_{ext}(r)$ by the laser field only with the simple form $D(r)=V_{ext}(r)=r$ in the length gauge. As long as $\psi_{El},\psi_{n'l'}$ are exact eigenfunctions of H the dipole operator may be expressed in a variety of different functional forms, which can be generated by the commutator $[H,\vec{r}]$. In [15] we showed that for the interpretation and an analytical approximation of the photo cross section the most valuable form for the dipole operator is given by the so-called acceleration gauge $\vec{D}=\vec{\nabla}V/\omega^2$, which expresses the dipole interaction as a force supplying the necessary recoil for the electron momentum generated by the ionization process. With this form of the dipole operator Eq. (2) reads

$$\sigma_{El\leftarrow n'l'}(\omega)=\frac{(2\pi)^2\alpha_F}{\omega^3}\times\frac{l_>}{2l'+1}|\langle\psi_{El}(r)|\partial_r V(r)|\psi_{n'l'}(r)\rangle_r|^2, \tag{3}$$

where V is the effective single-particle potential.

A first insight into the analytic structure of the cross section can be gained by considering a box potential as effective single-particle cluster potential. The derivative of the potential yields a δ function in the radial coordinate at $r=L$, where L is the radius of the cluster and the square of the matrix element in Eq. (3) collapses to a term proportional to $|\psi_f(L)|^2$. For high-photon energies the final wave function is well approximated by a free-particle wave function proportional to a cosine and the cross section oscillates as a function of the photon energy. Hence, using the acceleration

gauge for the dipole operator, the oscillation of the cross section is almost trivially understood for this case.

The single-particle potential originating from DFT calculations has a soft edge, which is modeled in the Woods-Saxon potential of Eq. (1) by the parameter a. Using WKB wave functions for the bound and continuum electron states and evaluating the integral of the matrix element Eq. (3) by the method of stationary phase leads to a simple expression for the ionization cross section. It depends merely on the effective single-particle potential and on the wave-number k of the continuum wave function inside this potential. Because the ionization energy of the electrons can be approximated by $-V_0/2$, the wave number in the potential range turns out to be

$$k=\sqrt{2\omega+V_0}. \tag{4}$$

The final analytical approximation for the cross section reads

$$\sigma(\omega)=D\frac{R(k)}{\omega^{7/2}}e^{-2a\pi k}[1+\beta\cos(2kL-\gamma)], \tag{5}$$

where D, R, β, and γ depend on the shape of the potential and a,L give the steepness of the potential edge and the radius of the Woods-Saxon potential. The details are given in [6].

The interesting aspect of Eq. (5) is the oscillation of the cross section as a function of the wave-number k of the ionized electron with frequency $2L$ and the exponential decay of the cross section with $-2a\pi k$. However, this result is only valid for the high-energy regime as discussed above because Eq. (5) has been derived within the single-particle picture.

B. Inclusion of collective effects by random phase approximation

If collective effects are important, i.e., for low excitation energies, the single-particle picture is not valid and an alternative approach has to be considered. Generally, there is a number of ways to include the collective effects in the calculation. First, there is the RPA in a formulation where a number of eigenfrequencies of an interacting system of single-particle states is determined by a matrix diagonalization within a linear approximation [16,17]. The absorption spectrum is then calculated by means of the matrix element in Eq. (2) for the wave function of the interacting many-particle system in the ground state, and the respective excited state which corresponds to an eigenfrequency of the collective electronic motion. The number of single-particle levels included in the calculation determines the number of eigenfrequencies. However, for ionization one is interested in a continuous cross section that requires a continuous spectrum as a function of energy instead of peaks at isolated resonance frequencies. This can be obtained with an RPA formulation by means of the polarization propagator of the system.

The polarization propagator $\Pi(\vec{r},t,\vec{r}',t')$ gives the linear response of a system to an external perturbation. The density variation of the ground state under the perturbation $V_{ext}(\vec{r},t)$ can be expressed as [18]

$$\delta\rho(\vec{r},t)=\int_{-\infty}^{t}dt'\int d\vec{r}'\,\Pi(\vec{r},t,\vec{r}',t')V_{ext}(\vec{r}',t'). \tag{6}$$

The propagator is equivalent to the retarded density-density correlation function [18]

$$\Pi(\vec{r}',t',\vec{r},t)=-i\,\theta(t-t')\times\langle\psi_0|[e^{iHt}\hat{\rho}(\vec{r})e^{-iHt},e^{iHt'}\hat{\rho}(\vec{r}')e^{-iHt'}]|\psi_0\rangle, \tag{7}$$

with the correlated ground state $|\psi_0\rangle$ of the valence electrons in single-particle representation, the full Hamiltonian H and with the density operator

$$\hat{\rho}(\vec{r})=\sum_i\delta(\vec{r}-\vec{r}_i), \tag{8}$$

where the index i runs over the number of particles of the system. The linear polarization of the system in z direction is the integrated density variation weighted by z,

$$\alpha(t)=-\int d\vec{r}\,\delta\rho(\vec{r},t)z. \tag{9}$$

The Fourier transform of $\alpha(t)$ is related to the photo cross section by [5]

$$\sigma(\omega)=4\pi\omega\alpha_F\,\mathrm{Im}[\alpha(\omega)]. \tag{10}$$

The polarization propagator Π can be calculated within the RPA resulting in an integral equation for Π [18]. The rather involved derivation, however, yields the same expression for Π as the TDLDA [19], which is pursued here. The polarization propagator from Eq. (7) without interaction among the valence electrons can be expressed by means of the single-particle Green's function $G(\vec{r},\vec{r}',E)$ in energy representation,

$$\Pi_0(\vec{r},\vec{r}',\omega)=\sum_i[\phi_i^*(\vec{r})\phi_i(\vec{r}')G(\vec{r},\vec{r}',E_i+\omega)+\phi_i^*(\vec{r})\phi_i(\vec{r}')G(\vec{r},\vec{r}',E_i-\omega)], \tag{11}$$

where the sum runs over all occupied single-particle states with eigenfunctions ϕ_i and eigenenergies E_i. An imaginary part ϵ is added to the energy ω to give a width to the resonances in the spectrum.

In order to determine the polarization propagator Π from Π_0 the linear response of the density ρ of the system to a perturbation is constructed explicitly. The external perturbation V_{ext} consists in the case of laserlight, linearly polarized along the $\hat{z}$ axis, of the potential $V_{ext}(\vec{r},t)=z\exp(-i\omega t)$. For noninteracting particles the perturbation of the ground-state density can be expressed in the energy representation as [5]

$$\delta\rho(\vec{r},\omega)=\int d\vec{r}'\,\Pi_0(\vec{r},\vec{r}',\omega)V_{ext}(\vec{r}',\omega)\equiv\Pi_0V_{ext}, \tag{12}$$

with

$$V_{ext}(\vec{r},\omega)=\int_{-\infty}^{\infty} dt e^{i\omega t} V_{ext}(\vec{r},t). \tag{13}$$

In the case of linearly polarized light we simply have $V_{ext}(\vec{r},\omega)=z$. Taking into account the interaction of the electrons leads to an additional perturbation, which depends itself on the density variation $\delta\rho$. This perturbation induces a potential approximated by

$$V_{ind}(\vec{r},\omega)=\int d\vec{r}'\left(\frac{1}{|\vec{r}-\vec{r}'|}+\frac{\mathrm{d}V_{xc}[\rho(\vec{r}')]}{\mathrm{d}\rho(\vec{r}')}\right)\delta\rho(\vec{r}',\omega)$$
$$\equiv V\delta\rho, \tag{14}$$

where the first part is due to the Coulomb interaction and the second part is determined by the exchange-correlation energy functional V_{xc} in the local-density approximation; for details see [20]. The density variation including the interaction among the electrons is obtained by adding V_{ind} to V_{ext} in Eq. (12). The resulting integral equation for the density variation reads in symbolic notation,

$$\delta\rho=\Pi_0 V_{ext}+\Pi_0 V\delta\rho. \tag{15}$$

To solve Eq. (15) the density variation $\delta\rho^*$ must be found, which is a fixed point of Eq. (15). This can be achieved, e.g., by calculating $\delta\rho$ self-consistently [19]. Alternatively, the equation can be explicitly solved for $\delta\rho$,

$$\delta\rho=(1-\Pi_0 V)^{-1}\Pi_0 V_{ext}\equiv\Pi V_{ext}. \tag{16}$$

In this formulation $\delta\rho$ includes the interaction among the electrons that occurs when the ground-state density is perturbed and is equivalent to $\delta\rho$ from RPA calculations. Using Eq. (16) in Eq. (9) the photoabsorption cross section Eq. (10) can be calculated for each desired energy in a discrete coordinate space representation once the matrix $(1+\Pi_0 V)$ has been inverted numerically [21]. For a comparison of the different schemes mentioned above, see [22].

To calculate the photo*ionization* cross section from the collective response of the valence electron cloud we have to find the effective perturbation $V_{eff}(r)$ representing the dipole operator in Eq. (2) for this case. From the case without collective interaction we know that V_{ext} is linked to the density variation through the polarization propagator Π_0 [see Eq. (12)]. For Eq. (2) to hold under collective interaction we must determine the effective perturbation from the very same form of the density variation as in Eq. (12), i.e., we demand

$$\delta\rho=\Pi_0 V_{eff}. \tag{17}$$

Comparison with Eq. (16) shows that

$$V_{eff}=V_{ext}+V\delta\rho=(1+V\Pi)V_{ext}. \tag{18}$$

The formulation in terms of an effective potential allows one to compare the cross sections for photoionization in the single-particle and the collective description simply and directly. The difference between the two approaches lies in the difference between the dipole operators, which is equal to $V_{ind}=V\delta\rho$ from Eq. (14). Since V_{ind} is proportional to the density variation $\delta\rho$ one sees immediately that the single-particle description does not differ much from the RPA result if $\delta\rho$ is small. For high frequencies of the perturbing field the electron cloud can not follow the rapid oscillations and $\delta\rho$ is bound to be small, thus leading to the equivalence of the single-particle and the collective picture for high-photon energies.

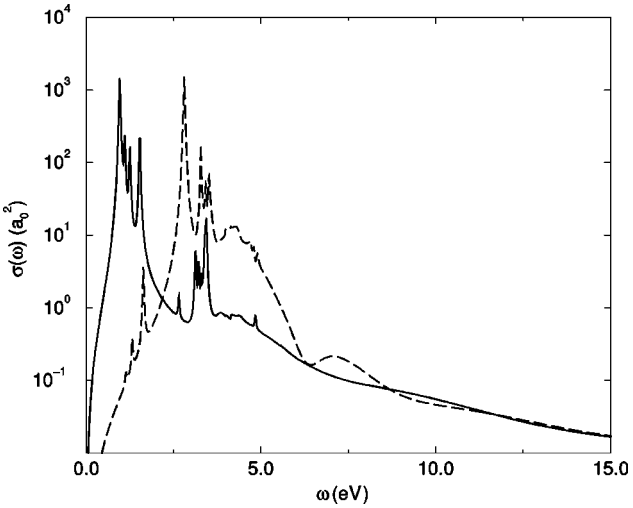

FIG. 2. Total absorption cross section as a function of the photon energy for the DFT potential from Fig. 1. The single-particle result is displayed by a solid line and the RPA result by a dashed line. The calculation was carried out with an imaginary part $\epsilon=0.04$ eV of the energy in Eq. (11).

III. COLLECTIVE VERSUS SINGLE-PARTICLE CROSS SECTION

Having provided the tools for the calculation of the collective and the single-particle photo cross section we are now able to compare both results to assess the energy range in which the single-particle approach is a valid approximation. The explicit calculations have been developed along the lines of the numerical implementation by Bertsch [21] but include a more accurate numerical calculation of the wave functions. High-precision wave functions for the single-particle electronic states are required in a numerical calculation of the absorption cross section for high-photon energies, as the cross section depends crucially on the wave functions at large radii.

In Fig. 2 we present the total photoabsorption cross section for Na_{34} based on the DFT potential from Fig. 1. The resonances in the spectrum have been broadened by an imaginary energy of $\epsilon=0.04$ eV inserted in Eq. (11). The absorption cross sections from the single-particle calculation (solid line) and from the RPA calculation (dashed line) differ significantly for photon energies up to approximately 10 eV. A pronounced plasmon peak develops in the RPA calculation, whereas in the single-particle calculation single-particle excitations appear. For energies higher than about 15 eV the cross sections clearly merge. The dipole sum rule, which serves as a numerical check, is fulfilled in this calculation to better than one percent.

Proceeding further to the ionization cross sections we begin with the ionization of a specific bound electronic level $n'l'$. The cross section for a transition from the given bound

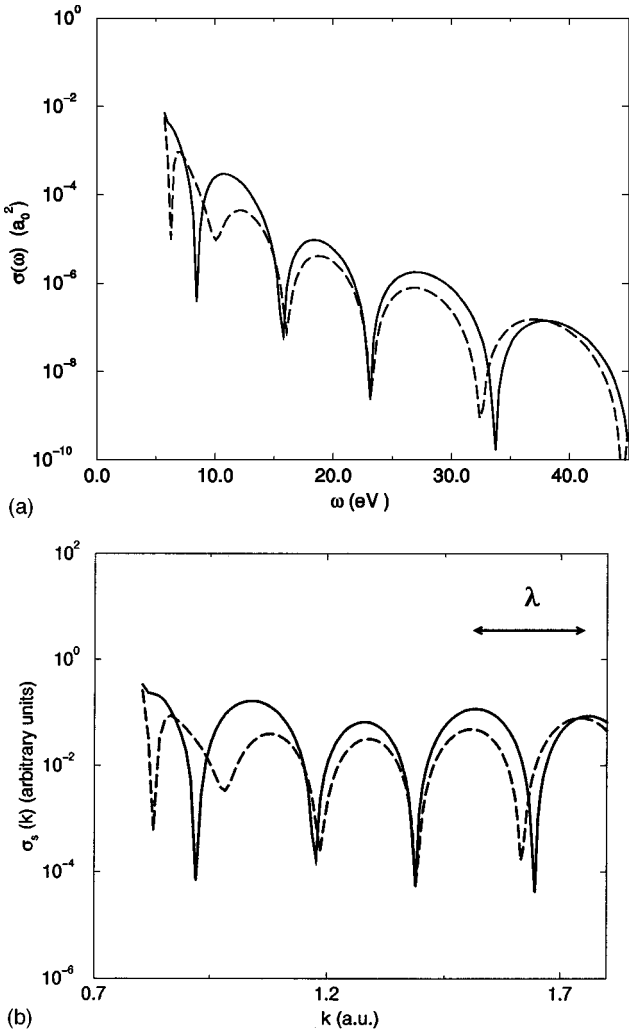

FIG. 3. The differential cross section for photoionization from the 1s level of the DFT potential in Fig. 1 in the single-particle approximation (solid line) and within RPA (dashed line). The imaginary part of the energy is $\epsilon = 0.0004$ eV. Part (a) shows the dependence of the photon energy ω and part (b) shows that the cross section is plotted versus the wave number $k = \sqrt{2\omega + V_0}$ of the ionized electron and $\sigma(k)$ has been scaled with the factor $k^7 \exp(2a\pi k)/(1+a^2k^2)$ to compensate for the global decrease. The arrow gives the oscillation frequency or wavelength in k space $\lambda = 2\pi/2L$.

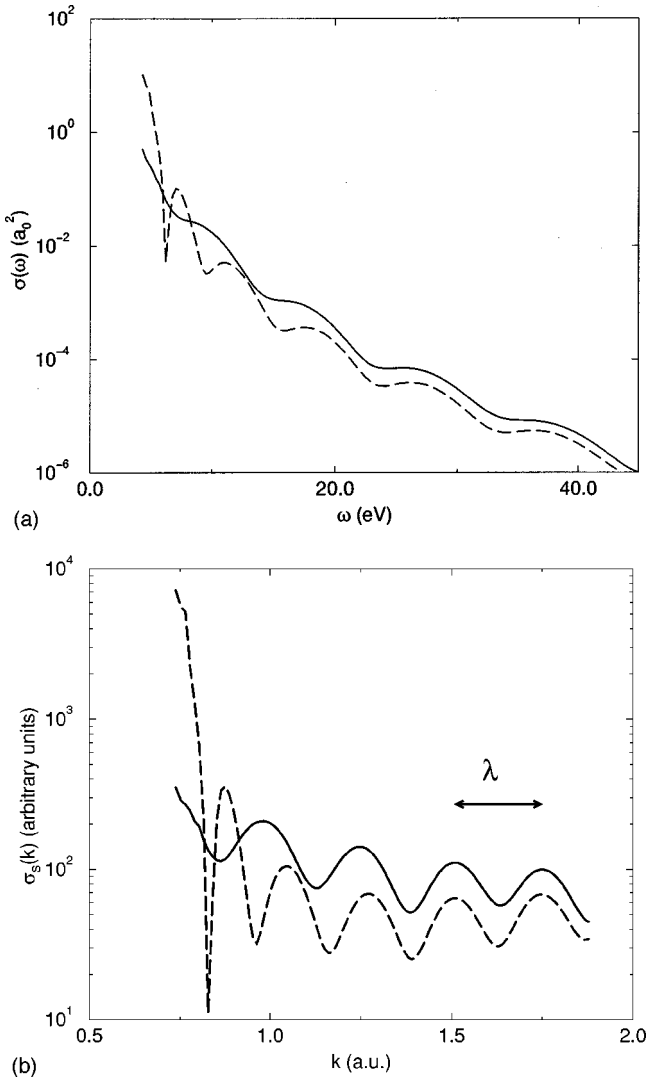

FIG. 4. Same as in Fig. 3 but for the total photoionization cross section from the bound levels of the DFT potential in Fig. 1.

state to an ionized state of a certain energy has to be calculated using the dipole operator D, see Eq. (2). As discussed in the previous section, in the single-particle calculation $D = r$ containing only the external perturbation while for interacting electrons within the RPA we have $D = V_{eff}$ from Eq. (18), which represents the collective response of the electron cloud to the oscillating electromagnetic field. The result is shown in Fig. 3 for the transition from the 1s level with energy E_i to p states with energy $E_p = \omega + E_i$. For higher-photon energies the cross sections merge although they become not entirely identical. However, the main characteristics of the cross section that were predicted analytically are visible in both, the single-particle and the RPA calculations. A pronounced oscillation with a frequency equal to the diameter of the cluster and an overall exponential decay of the cross section can be identified. This behavior of the cross sections can be clearly demonstrated if the cross section, scaled with respect to the exponential decay extracted from the semiclassical analysis as summarized in Sec. II A, is plotted as a function of the wave number of the ionized electron, see Fig. 3(b).

Finally, we present the total photoionization cross section in Fig. 4. Again, the single particle and RPA cross sections merge although they become not identical with increasing photon energy. However, the oscillations are even better in phase than in the partial cross sections of Fig. 3. The common oscillatory structure is clearly visible and the corresponding wavelength agrees with the value analytically calculated in Sec. II A and shown in Fig. 4(b) for comparison.

Most importantly for a possible experimental extraction of the cluster radius from the photoionization cross section, we can read off from Fig. 4 that the cross section from an energy starting as low as about 10 eV can be used to determine the oscillation frequency, despite the presence of collective electronic behavior (dashed line).

Finally we note that according to our numerically obtained cross sections details of the potential affect the absolute value, the absolute positions of the extrema, and the

decrease of the cross section, but not the oscillation frequency. Therefore, we are led to the conclusion that the oscillations will be observable in the experiment and that they provide direct information about the cluster radius in agreement with theoretical predictions. This should be the case, even if the theoretical ionization cross section, dependent on the form of the single-particle potential, does not very well agree with the experimental cross section.

IV. CONCLUSIONS

We have shown that the cross section for photoionization of alkali-metal clusters can be adequately accounted for by calculations in the single-particle picture neglecting collective effects if the photon energy is higher than a certain critical energy. For the cluster Na_{34} this energy turns out to be of the order of 15 eV. Beyond this photon energy the cross sections calculated in the single-particle approximation and with RPA merge and they display a pronounced oscillation as well as an exponential decrease as a function of the wave number of the ionized electron. The decrease and the oscillation can be derived by means of a semiclassical analysis that relates the cluster diameter and the steepness of the potential edge to the oscillation frequency and to the exponential decrease, respectively. The RPA calculation preformed here shows that the oscillatory structure in the ionization cross section appears already close to the ionization threshold where the ionization yield is still relatively large and an experimental verification should be possible in the future.

ACKNOWLEDGMENTS

We gratefully acknowledge financial support by the Deutsche Forschungsgemeinschaft, within the SFB 276, located at Freiburg. We also thank the U.S. Department of Energy's Institute for Nuclear Theory at the University of Washington for its hospitality and for partial support during the completion of this work.

[1] M. Brack, Rev. Mod. Phys. **65**, 677 (1993).
[2] W. A. deHeer, Rev. Mod. Phys. **65**, 611 (1993).
[3] C. Bréchignac and J. P. Connerade, J. Phys. B **27**, 3795 (1994).
[4] C. Guet and W. R. Johnson, Phys. Rev. B **45**, 11 283 (1992).
[5] W. Ekardt, Phys. Rev. B **31**, 6360 (1985).
[6] O. Frank and J. M. Rost, Z. Phys. D **38**, 59 (1996).
[7] O. Frank and J. M. Rost, Chem. Phys. Lett. **271**, 367 (1997).
[8] P. J. Benning *et al.*, Phys. Rev. B **44**, 1962 (1991).
[9] T. Liebsch, R. Hentges, J. Viefhaus, U. Becker, and R. Schlog, Chem. Phys. Lett. **279**, 197 (1997).
[10] Y. B. Xu, M. Q. Tan, and U. Becker, Phys. Rev. Lett. **76**, 3538 (1996).
[11] S. Keller, E. Engel, H. Ast, and R. M. Dreizler, J. Phys. B **30**, L703 (1997).
[12] R. O. Jones, in *Clusters of Atoms and Molecules*, edited by H. Haberland (Springer-Verlag, Berlin, 1994).
[13] W. Ekardt, Phys. Rev. B **29**, 1558 (1984).
[14] H. Friedrich, *Theoretische Atomphysik* (Springer-Verlag, Berlin, 1990).
[15] O. Frank and J. M. Rost, Comments At. Mol. Phys. **34**, 1 (1998).
[16] D. J. Rowe, Rev. Mod. Phys. **40**, 153 (1968).
[17] C. Yannouleas and R. A. Broglia, Phys. Rev. A **44**, 5793 (1991).
[18] E. K. U. Gross and E. Runge, *Vielteilchentheorie* (Teubner, Leipzig, 1986).
[19] A. Zangwill and P. Soven, Phys. Rev. A **21**, 1561 (1980).
[20] O. Gunnarsson and B. I. Lundqvist, Phys. Rev. B **13**, 4274 (1976).
[21] G. Bertsch, Comput. Phys. Commun. **60**, 247 (1990).
[22] M. Madjet, C. Guet, and W. R. Johnson, Phys. Rev. A **51**, 1327 (1995).